JOURNAL OF PROPULSION AND POWER
Vol. 9, No. 2, March–April 1993

Numerical Simulations of Gas Turbine Combustor Flows

D. Lee* and C. L. Yeh†
National Cheng Kung University, Tainan, Taiwan, Republic of China
and
Y. M. Tsuei‡ and J. Chou§
Chung-Shan Institute of Science and Technology, Taipei, Taiwan, Republic of China

A general two-dimensional computer code has been developed for simulating gas turbine combustor flow. The code employs a nonstaggered body-fitted coordinate system and the SIMPLE algorithm with power law or second-order upwind scheme for the convective terms. Several turbulence models have been implemented and compared. For the reacting cases, three combustion models—the laminar combustion model, the fast chemistry with the assumed probability density function model (pdf), and the eddy breakup (EBU) model—have been used. The use of the zonal grid and the adaptive grid methods have also been demonstrated in the selected cases. This code can be conveniently applied to many other internal fluid flow or heat transfer problems.

Nomenclature

A = coefficients in discretized equation
C_i = constants in turbulence models
C_t = coupling factor for the weight function
f = conserved scalar
G = generation rate of k
g = Jacobian squared or the variance of the f
g^{jk} = metric tensor
k = turbulence kinetic energy
P = probability density function
q^j, q^k = general coordinate
R = source term before transformation
Re = Reynolds number
S = lumped source term after transformation
U, V = contravariant velocity
u = Heaviside step function
V^j = contravariant velocity
W = weight function
Γ^Φ = effective diffusion coefficient for the variable Φ
δ = dirac delta
ε = dissipation rate
ξ, η = general coordinates
π = density
Φ = variables
ω = dominant rate in EBU model

Introduction

THE rapid growth in computing power and storage capacity of the digital computer has provided a strong motivation for numerically simulating flows to complement or even substitute traditionally experimental approaches of gas turbine combustor flows. There have been a few state-of-the-art codes in existence in the gas turbine combustor research and development community. CONCERT of GE,[1] PACE from Rolls Royce,[2] and PREACH of Pratt and Whitney[3] are examples among others.

With the CONCERT code, GE is now able to produce practically useful results from three-dimensional flow computations. An example is the prediction for the flowfield of a sector of a three-dimensional gas turbine combustor with dilution holes and cooling film slots.[1] The PACE program of Rolls Royce has been applied to a number of development and production gas turbine combustor geometries, both tubular and annular. Examples are the prediction of flow of a 20-deg sector combustor with symmetry conditions applied on the circumferential end planes and the dump diffuser flow computations.[2] These results have been used to improve combustor pattern factor and cooling device design, as well as in optimizing the diffuser flow and loss. Although no specific examples of use were given in Ref. 3, it was stated that the code used in the gas turbine combustor is currently a useful design and development tool, and this usefulness is increasing.

Features of the above codes are tabulated in Table 1. All three programs employ the SIMPLE-type algorithm and the staggered grid system. As far as the coordinate system is concerned, only CONCERT utilizes the nonorthogonal body-fitted coordinate system which has greater flexibility in handling curved boundaries; it is also equipped with the zonal grid method to resolve the geometrical complexity, such as the dilution holes and cooling slots. With regard to physical submodels, the k-ε turbulence and fast chemistry combustion models with assumed pdf are the most widely adopted models. In Ref. 2, although the combustion model used is not specifically mentioned, transport equations with formation rate as source term has been used in predicting the nitric oxide emission levels. Some numerical aspects such as numerical schemes, gridding techniques, and convergence rate have been discussed by Shyy et al.[1,4]

In this study, a numerical tool suitable for predicting gas turbine combustor flows has been independently developed by the authors. As a result, a package of two-dimensional computer code has been produced. This code is based on the SIMPLE algorithm with a nonstaggered body-fitted coordinate system. The finite-difference operator is either the power law scheme or the second-order upwind scheme. Three turbulence models—the k-ε model,[5] the Reynolds stress model (RSM),[6] and the Algebraic stress model (ASM)[7]—and the two derivatives of the k-ε model[8,9] have been used. The laminar combustion model,[10,11] the fast chemistry with assumed pdf,[11,12] as well as the eddy breakup models[13,14] are used in the calculation of reacting combustor flows. For the isothermal flow computations, the test problems included are the backward-facing step flow and the contoured wall combustor

Presented as Paper 90-2305 at the AIAA/SAE/ASME/ASEE 26th Joint Propulsion Conference, Orlando, FL, July 16–18, 1990; received Jan. 14, 1991; revision received Aug. 29, 1992; accepted for publication Sept. 24, 1992.

*Associate Professor, Institute of Aeronautics and Astronautics.
†Graduate Student, Institute of Aeronautics and Astonautics.
‡Research Scientist, Aeronautical Research Laboratory.
§Senior Research Scientist, Aeronautical Research Laboratory.

Table 1 Features of various industrial codes

Code	Algorithm	Finite-difference operator	Grid	Turbulence model	Chemistry model	Other
CONCERT	SIMPLE	SOUS	Staggered Body-fitted Zonal	k-ε Model	Fast chemistry with assumed PDF	Multigrid
PACE	SIMPLE	QUICK	Staggered Orthogonal curvilinear Zonal	k-ε Model	——	——
PREACH	SIMPLE	Hybrid BSUDS	Staggered Cartesian Curvilinear orthogonal Multiregion	k-ε Model	Laminar model Eddy breakup	——

with or without side jets. As for the computation of the reacting flows, axisymmetric sudden expansion combustor and the reacting flow of a two-ring flame stabilizer are used. The zonal grid method and the adaptive gridding technique have also been utilized in selected cases. Computational results are compared to experimental data whenever they are available. Brief discussions are given for each test case.

Numerical Aspects

The governing equations and the turbulence model equations can be expressed in the following unified form as

$$\frac{\partial}{\partial t}(\rho\Phi) + \text{div}(\rho V\Phi) = \text{div}(\Gamma^{\Phi}\,\text{grad}\,\Phi) + R^{\Phi} \qquad (1)$$

where Φ represents the dependent variable, Γ^{Φ} is the effective diffusion coefficient of variable Φ, and R^{Φ} is the source term for the equation. In order to handle the flowfields in complex geometries and to incorporate boundary conditions more conveniently and accurately, the equations are transformed to the non-orthogonal body-fitted coordinate system, and this leads to

$$\frac{\partial}{\partial t}(\sqrt{g}\rho\Phi) + \frac{\partial}{\partial q^j}(\sqrt{g}\rho V^j\Phi) = \frac{\partial}{\partial q^j}\left(\sqrt{g}g^{jk}\Gamma^{\Phi}\frac{\partial\Phi}{\partial q^k}\right) + \sqrt{g}R^{\Phi} \qquad (2)$$

For a two-dimensional, steady, incompressible flow, the governing equation becomes

$$\frac{\partial}{\partial\xi}(\sqrt{g}\rho U\Phi) + \frac{\partial}{\partial\eta}(\sqrt{g}\rho V\Phi) = \frac{\partial}{\partial\xi}\left(\sqrt{g}g^{11}\Gamma^{\Phi}\frac{\partial\Phi}{\partial\xi}\right) + \frac{\partial}{\partial\eta}\left(\sqrt{g}g^{22}\Gamma^{\Phi}\frac{\partial\Phi}{\partial\eta}\right) + S^{\Phi}$$

where

$$S^{\Phi} = \sqrt{g}R^{\Phi} + C^{\Phi}$$

$$C^{\Phi} = \frac{\partial}{\partial\xi}\left(\sqrt{g}g^{12}\Gamma^{\Phi}\frac{\partial\Phi}{\partial\eta}\right) + \frac{\partial}{\partial\eta}\left(\sqrt{g}g^{21}\Gamma^{\Phi}\frac{\partial\Phi}{\partial\xi}\right)$$

$$\sqrt{g} = x_{\xi}y_{\eta} - x_{\eta}y_{\xi} \qquad g^{12} = g^{21} = -(x_{\xi}x_{\eta} + y_{\xi}y_{\eta})/g$$

$$g^{11} = (x_{\eta}^2 + y_{\eta}^2)/g \qquad g^{22} = (x_{\xi}^2 + y_{\xi}^2)/g$$

$$U = (uy_{\eta} - vx_{\eta})/\sqrt{g} \qquad V = (vx_{\xi} - uy_{\xi})/\sqrt{g} \qquad (3)$$

Eq. (3) can be discretized by using various differencing schemes and the final form of discretized equation becomes

$$A_{\Phi}\Phi_{\Phi} = \sum_{i=E,W,N,S} A_i\Phi_i + S \qquad (4)$$

The discretized Eq. (4) along with a pressure correction equation can be formulated and solved with the SIMPLE algorithm.[15]

In the present study, the grid cell structure for the various physical variables is a nonstaggered system. All the physical variables are at the same node and share the same control volume. This may simplify the cell structure when the code is extended to a three-dimensional version. However, with this grid cell arrangement, numerical pressure oscillations may occur. To overcome this difficulty, Rhie and Chow[16] used the upwind scheme to discretize the pressure gradient term as is briefly described next. In the SIMPLE algorithm, the pressure correction equation is obtained by substituting the corrected contravariant velocities which include the pressure gradient terms into the continuity equation. It should be remembered that in a nonstaggered grid arrangement the contravariant velocities on the control surfaces are obtained by interpolations between grid nodes. These interpolations, in fact, represent the $2 - \Delta\xi$ difference scheme for the pressure gradient term and cannot sense the $1 - \Delta\xi$ pressure oscillation. As a remedy, the pressure gradient term in the corrected contravariant velocity is substituted by a local $1 - \Delta\xi$ difference scheme and thus avoid the difficulty. This scheme of Rhie and Chow is adopted in this study.

A two-dimensional grid generator LT-GRID[17] has been used to create the initial grid system. The grid generator is based on solving the elliptic equations[18] which govern the distribution of grids. The adaptive grid method and the zonal grid method have been applied in the present code to improve the solution accuracy and to further enhance the capability in handling complex geometries. The adaptive grid method employed here[19–21] is based on the concept of equidistribution of some weight functions. In this study, weight function assumes the form of

$$W_i = 1 + (\Phi_x)_i + \sum_{k=1,k\neq i}^{N} (\Phi_x)_k \times C_t(\exp^{-|i-k|}) \qquad (5)$$

where Φ_x is the gradient of selected flow property and C_t $(\exp^{-|i-k|})$ specifies the strength of coupling among neighboring weight functions. For example, if C_t is set to zero, then there will be no coupling among weight functions. For a nonzero C_t, the exponential decay of the coupling with respect to the distance from ith coordinate line is arbitrarily assumed. It is shown that with this coupling the grid can be smoother and in most cases can produce a more accurate solution.[21]

As discussed in Ref. 2, although the general nonorthogonal mesh does offer complete flexibility, a severely acute angle of geometry can still lead to difficulties within the solution algorithm and slow convergence. Therefore, the zonal grid method is appealing when the combustor geometry is complex (e.g., dilution holes, slots, gutter rings). With the zonal method, the physical domain of interest can be divided into several simple subdomains. With unified index notation and conservation across the boundaries, each subdomain can be solved separately and consistently by the same solver. At the same time, each subdomain has greater flexibility in the distributing

grid. In this study, the zonal grid method with conservative interpolation technique[22] is applied to a flameholder problem. More details can be found in Refs. 23 and 24.

Turbulence and Chemistry Models

Available turbulence and chemistry models suitable for computing turbulent reacting flows have been reviewed, e.g., by Jones and Whitelaw[25] and by Khalil.[26] It was concluded by Jones and Whitelaw that current turbulence and combustion models are able to calculate velocity, temperature, and major species with accuracy sufficient to guide experimental development. However, the capacity is basically "postdictive" rather than predictive.

In the present study the standard k-ε model and two of its derivatives, the algebraic stress model (ASM) and the Reynolds stress model (RSM) have been used and their performances have been documented. With regard to chemistry models, a laminar combustion model, a fast chemistry model with assumed pdf as well as an eddy breakup (EBU) model have been adopted. These physical submodels are briefly discussed in the following.

Turbulence Models

k-ε Model

Standard model. In the eddy-viscosity approach for turbulence modeling, the most popular choice is the k-ε model,[5] which solves the transport equations for the turbulence kinetic energy k and its dissipation rate ε. The transport equations for k and ε can be cast in the same form as Eq. (1). The diffusion coefficients and source terms are

$$\Gamma^k = \mu_{\text{eff}}/\sigma^k$$

$$R^k = G - \rho\varepsilon$$

for the k equation

$$\Gamma^\varepsilon = \mu_{\text{eff}}/\sigma^\varepsilon$$

$$R^\varepsilon = \varepsilon(C_1 G - C_2\rho\varepsilon)/k$$

for the ε equation

$$G = -\rho\overline{u_i u_j}\frac{\partial V_i}{\partial x_j} \tag{6}$$

where μ_{eff} is the effective viscosity and C_1, C_2 are constants.

Modified ε equation. In the computation of flows with recirculating zones, it is found that the k-ε model underestimates the size of the recirculation zone because the predicted G is too high. To correct this a modification of the ε equation is made by adding one term, $C_3(G^2/\rho\varepsilon - G)$, to the ε equation where C_3 is a constant, If G is too high the dissipation rate will raise accordingly, therefore, a more reasonable development of flow can be obtained due to the balance between k and ε.[8]

Modified C_μ. In the standard k-ε model, the coefficient C_μ embedded in μ_{eff} is taken as a constant. To consider the local turbulence strength, Rodi[7] suggested that a functional form of C_μ should be used. In our study the following dependence of C_μ on the ratio $G/\rho\varepsilon$[9] is used

$$C_\mu = \frac{2}{3}\frac{1-\alpha}{w}\frac{1-(1/w)[1-\alpha(G/\rho\varepsilon)]}{\{1+(1/w)[(G/\rho\varepsilon)-1]\}^2} \tag{7}$$

where w is around 2.5–2.8, and α is around 0.598–0.549.

RSM

In the RSM the transport equations for the Reynolds stresses are solved. These transport equations are derived directly from the Navier-Stokes equation.[6,27] The major difficulties in this model are the modeling of the pressure strain term and the third-order correlation term.[6] In the present study, model constants are taken from Amano et al.[28] Note that for a steady, two-dimensional case, in addition to the k and ε equations, there are three more equations that have to be solved for the components of the Reynolds stresses. At the present time RSM is the most general turbulence model, although the extra computational effort is a further drawback in addition to the aforementioned modeling difficulties.

ASM

Simplification of RSM to reduce the computational efforts is possible under certain conditions. Ljuboja and Rodi[7] assumed that the combination of convection and diffusion terms are either small or approximated by the algebraic form of $\overline{u_i u_j}$, the resulting transport equations then become algebraic. Since the derivation of ASM is based on some assumptions, only in those flow regions where the assumptions are satisfied, (e.g., where the transport of $\overline{u_i u_j}$ is not important) can ASM provide better results.

Chemistry Models

Laminar Combustion Model

In this model,[10,11] instantaneous reaction is assumed. The conserved scalar, i.e., the mixture fraction f is considered, and a transport equation for f is solved. The temperature and species can be obtained by using the linear relationship with f.

Fast Chemistry with Assumed pdf

In computing the turbulent reacting flows, the fluctuations of the conserved scalar f is taken into account by including the variance g of f in the formulation.[11,29] Once the mean and the variance of the conserved scalar are computed, the temperature and the other properties can be obtained from the convolution of the pdf. The mean $\tilde{f}$ and the variance g of the conserved scalar f are defined as

$$\tilde{f} = \int_0^1 fP(f)\,df \tag{8}$$

$$g = \int_0^1 (f-\tilde{f})^2 P(f)\,df \tag{9}$$

and note that

$$\int_0^1 P(f)\,df = 1 \tag{10}$$

Two assumed pdf are employed in the current study, the first is with battlement shape and the second is with triangular shape.[11,12] The mathematical expression for battlement shape pdf can be expressed as

$$P(f) = \alpha\delta(f^+) + (1-\alpha)\delta(f^-) \tag{11}$$

where $f^+ = \tilde{f} + \sqrt{g}$, $f^- = \tilde{f} - \sqrt{g}$. Equation (11) implies that the probability of f being f^+ is α, and the probability of f^- is $1-\alpha$. Since the values of f^+, f^- should be restricted between 0 and 1, α can be obtained in terms of $\tilde{f}$ and g by utilizing definitions in Eqs. (8–11). And together with the definition of the conserved scalar f, mean values of the other properties can be determined accordingly. In the second pdf, the expression for triangular shape pdf is

$$P(f) = C[u(f-f^-) - u(f-f^+)] \tag{12}$$

where u is the Heaviside step function and $C = 1/2\sqrt{3g}$, $f^+ = \tilde{f} + \sqrt{3g}$, $f^- = \tilde{f} - \sqrt{3g}$. The procedure of determining mean property values is similar to that of battlement shape pdf case.

EBU

The basic idea behind the EBU model[13,14] considers both the reaction rate R_{fu} (chemically controlled) and the eddies breakup rate R_{EBU} (diffusionally controlled). The dominant rate ω will be the minimum of reaction rate R_{fu} and eddies breakup rate R_{EBU}, i.e.

$$\begin{aligned} \omega &= \min(R_{fu}, R_{\mathrm{EBU}}) \\ R_{fu} &= A_0 \bar{\rho} \overline{Y_F Y_O} \exp(-E/R\tilde{T}) \\ R_{\mathrm{EBU}} &= C\bar{\rho}(\varepsilon/k)\sqrt{g_F} \\ g_F &= (Y_F - \tilde{Y}_F)^2 \end{aligned} \tag{13}$$

where the overbar stands for the mean values, Y_F is the mass fraction of fuel, Y_O is that of oxidizer and A_0 and C are constants. This dominant rate ω is then included in the source term of the transport equation for $\tilde{Y}_F$. With computed values of $\tilde{Y}_F$ and its variance, the other properties can be determined by following a similar procedure to that mentioned in the previous models. Note that battlement shape pdf is employed in this model.

Results and Discussions

Calculations of various two-dimensional flows in different geometries have been performed. Since most of the available experimental data are published with regular geometries, our test problems therefore include geometries such as a confined backward-facing step and a sudden expansion pipe for the validation of our computer code. The other geometries considered include a contoured wall combustor, a slinger-shape combustor, and a channel with triangular block in the stream. The numerical solutions are compared to those of experimental results whenever they are available.

Backward-Facing Step

This case has been used to demonstrate the performance of various turbulence models. The step height in the problem is one-ninth of the total height of the channel, and the computational domain length extends up to 36 times of the step height. In this test case, the inlet velocity and k profiles were taken from the measurements.[30] The boundary condition for ε is assumed to be a uniform distribution. The calculation is performed on a VAX 8600 computer with grid of 121 × 51, and $Re = 3.2 \times 10^4$. This grid number is believed to be fine enough to yield grid-independent solution. The mean velocity profiles are very close to each other, this is seen in Fig. 1. It is found that the mean velocity profiles are insensitive to the variation of the models as well as the inlet conditions. This also implies that good prediction of the mean velocity profile may be misleading in the sense that at the same time turbulence details can be far from each other. As far as the turbulence kinetic energy is concerned, Fig. 2 shows the performance of each model using the uniform inlet ε profile at three different streamwise locations in the recirculating region (2H), reattaching region (6H), and the redeveloping region (8H), respectively. It is seen that the standard k-ε, ASM, and RSM models perform similarly. On the other hand, the k-ε with modified ε and k-ε with modified C_μ perform differently and the former provides the best results in the recirculation zone. However, it also tends to overpredict the dissipation rate in the downstream and results in a longer reattachment length. It is found that the inlet boundary conditions significantly altered the detailed structure of the turbulence.[31]

The fact that the performance of a turbulence model varies from one region to another may prompt the need for the zonal method of turbulence model advocated by Ferziger and his co-workers.[32,33] Should this idea be adopted, care should be taken in choosing the "best" model which is specifically suitable to each zone. At the present stage, in industrial codes the k-ε models remain in widespread use in spite of their weakness.

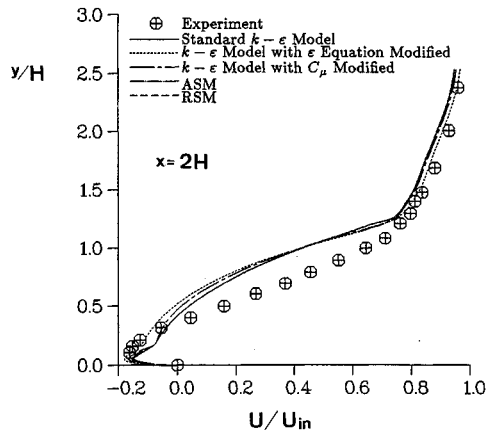

Fig. 1 Streamwise mean velocity profiles.

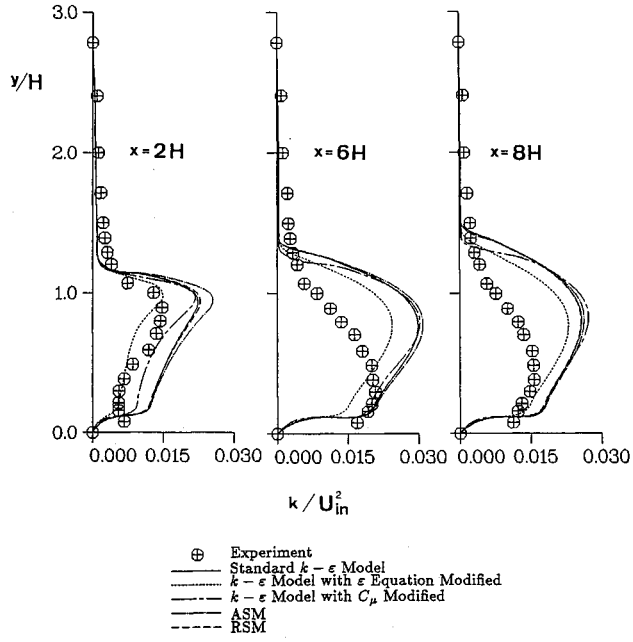

Fig. 2 Turbulence kinetic energy profiles at x = 2H, 6H, and 8H.

Contoured Wall Combustors

The second problem considered is a planar two-dimensional contoured chamber flow with grid layout as shown in Fig. 3. The Reynolds number based on the inlet height and velocity is 2.6×10^4. Figure 4 shows the streamlines of this flow and the size of the recirculation zone is found to be about the same to the experimental data. In Fig. 5, the mean velocity profiles at five locations are compared with the experimental data.[34] In this calculation, the measured inlet velocity and k profiles are employed for the inlet boundary conditions. It is found that the predicted mean velocity profiles of different turbulence models present no significant difference among each other. Therefore, only the standard k-ε model is used for the rest of the computations. A very close match between the predictions and the measurements is achieved near the outlet of the flow. The deviations from experimental results in the middle part of the test section may be attributed to the accuracy of the turbulence model and to the inadequate prescription of the inlet ε levels. In Fig. 6, the comparison is made between the predicted and measured values of the turbulence kinetic energy. The trend is, in general, agreeable except that the location of the peaks is not correct quantitatively.

In a practical combustor, an excessively high temperature is detrimental to the turbine blades, therefore, dilution jets are devised to lower the temperature. A dilution jet is a type

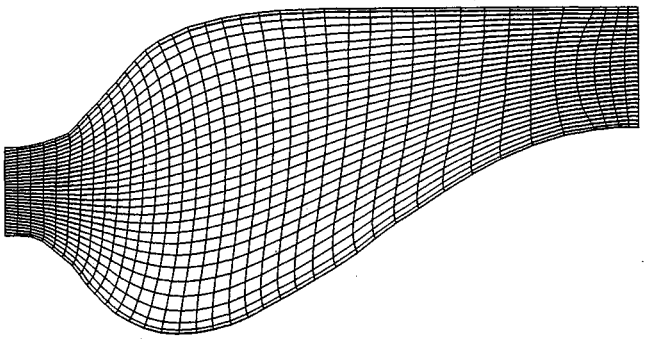

Fig. 3 Grid for the contoured wall combustor.

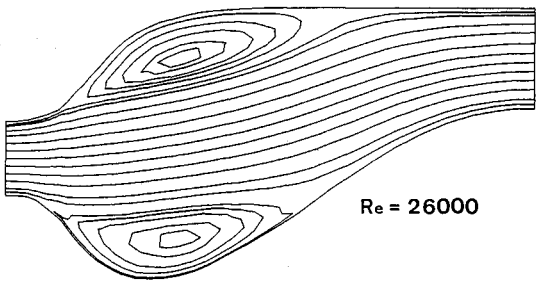

Fig. 4 Streamlines of the combustor flows.

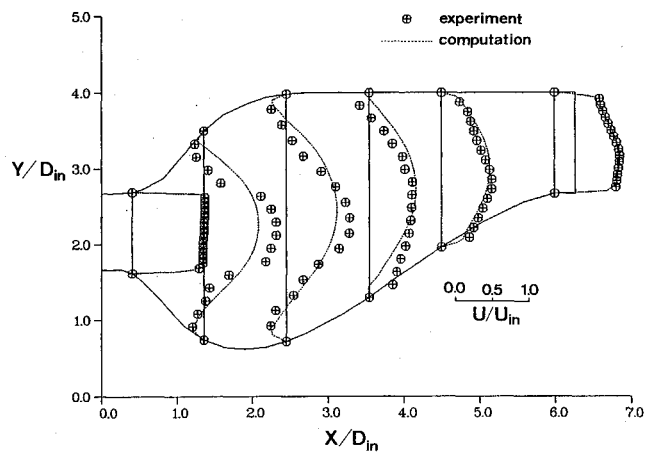

Fig. 5 Mean velocity profiles.

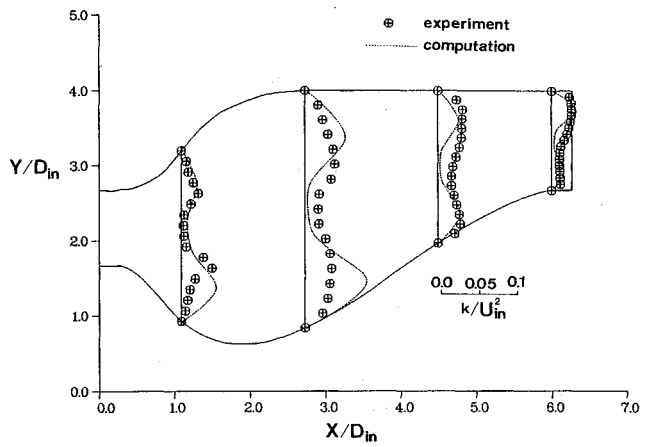

Fig. 6 Comparison of the predicted and measured values of the turbulence kinetic energy.

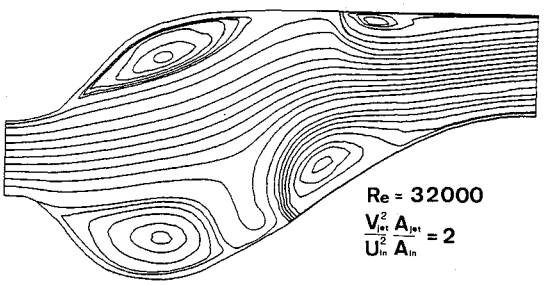

Fig. 7 Streamlines with dilution jets.

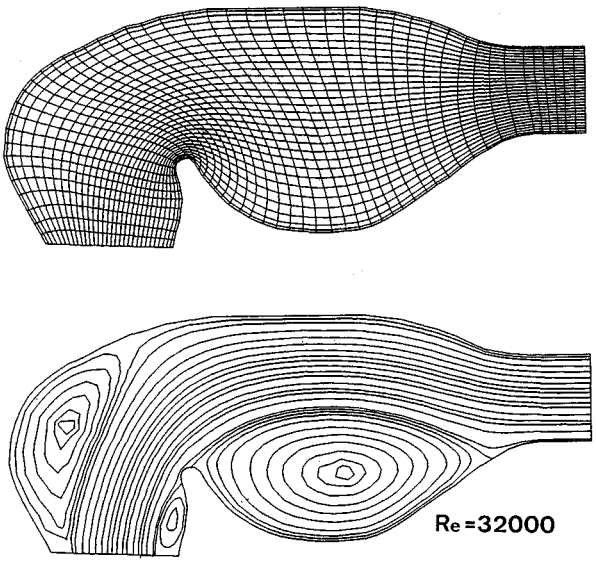

Fig. 8 Grid and streamlines of a slinger-shape combustor.

of side-jet flows of medium velocity ratios and its influence on the entire flowfield can be large.[35] In the two-dimensional cases, recirculation zones are formed behind the dilution jets, and their sizes depend on the momentum flux ratio of the jets to the main stream, i.e., $V_{jet}^2 b/U_{in}^2 B$, where b is the jet width and B the inlet height. The dilution jets divide the original recirculation zones into several parts, the recirculation zones before the jets are largely not affected by the jets unless the blocking effect of the dilution jets is large. While the recirculation zones behind the jets become larger as the jet velocity increases. Momentum flux ratios between 0–2 have been calculated. In Fig. 7, the results with $Re = 3.2 \times 10^4$ is shown. Recirculation bubbles behind the dilution jets are clearly seen.

Another test case in this category as shown in Fig. 8 is the streamlines of a slinger-shape chamber which is a simplified combustor model for some of the helicopter power plants. This case is intended to demonstrate the capability of the current code in handling larger curvature geometry. The case is computed with $Re = 3.2 \times 10^4$.

Reacting Flow in a Sudden Expansion Pipe

In the reacting cases, the three combustion models, i.e., the laminar combustion model, the fast chemistry with assumed pdf, and the eddy breakup model, have been incorporated into the code. The flowfield of an axisymmetric, sudden expansion can combustor is computed. The combustor configuration, detailed specifications, and boundary conditions are referred to by Lewis and Smoot.[36] The results obtained here are also compared to their experimental data. In addition to the model testing, the adaptive grid method has been implemented with the laminar combustion model and the effectiveness of the method is evaluated. The k-ε turbulence model is used in this computation. Figure 9 shows the variation of mixture fraction f along the axial position, where model 1 is the laminar combustion model, model 2a is the fast chemistry with pdf of battlement shape, model 2b is with pdf of triangular shape, and model 3 is the EBU model. It is seen that variance of conserved scalar has significant effect

on the prediction values. Also shown in the next figure is the adaptive solution of model 1. The adaptive grid in this computation is shown in Fig. 10a. It is interesting to note that the grid itself shows the trace of flame front. Fig. 10b clearly demonstrates the effectiveness of the adaptive grid method. For the uniform grid solution, doubling the grid in each direction does not improve the solution much. On the other hand with the adaptive grid method, solution mimics the experimental data more closely. From the results of the above figure, it can be stated that grid can be an important issue in predicting the reactive flow.

Flameholding Flows

In this part the reacting flows of flame stabilizer are computed. Two cases are studied, the first is a wedge flow in a duct and the second is flows of a two-ring flame stabilizer. The zonal grid method is employed to treat the complex geometries due to the flame stabilizer. The eddy breakup combustion model is used for the calculations. The first case is intended to validate the code and to provide more comparison between the predictions and the experimental data for reacting cases. The configuration and the flow conditions of the wedge flow are referred to Fujii and Eguchi[37] and Lee and Yeh.[24] Since the details are reported in Ref. 24, only one result will be given here to demonstrate the usefulness of the current code. Figure 11 demonstrates the axial velocities along the symmetry plane in the recirculation zone. The velocity is normalized by the maximum reverse flow velocity U_{ref} and the axial distance is normalized by the recirculation bubble length L_{rz}. These normalizations yield a good similarity among the curves. The agreement to the experimental results is fairly good.

The grid for the two-ring flame stabilizer is shown in Fig. 12, where the blockage ratio is 0.4, θ angle is 60 deg, and Re = 32,000. The computational domain is divided along the base of the flame stabilizer to two subdomains. In Fig. 13, the temperature distribution obtained by using the EBU combustion model and the equivalence ratio of unity is shown. The shaded area is the region which attains the highest temperature. Note that this shaded area originates from the recirculation zone and covers most of the central part of the tube.

In this part, we have demonstrated the utilization of the zonal grid method, physics of the flow is not explored in details. For a complex geometry flow, the zonal grid method should prove to be more robust than other grid generation methods.

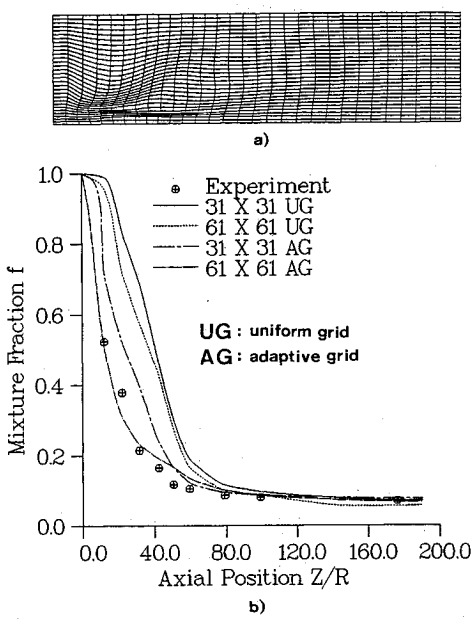

Fig. 10 Grid and adaptive solutions for the mixture fraction f along the axis. a) Adaptive grid, b) effectiveness of the adaptive grid.

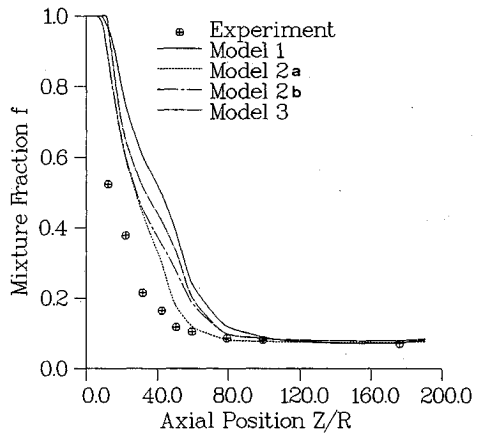

Fig. 9 Variation of mixture fraction f along the axis.

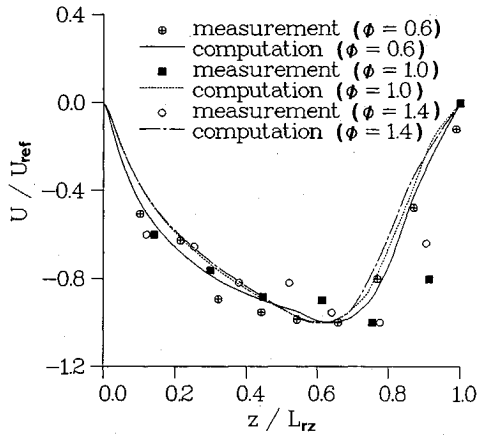

Fig. 11 Axial velocity in the recirculation zone of a wedge flow.

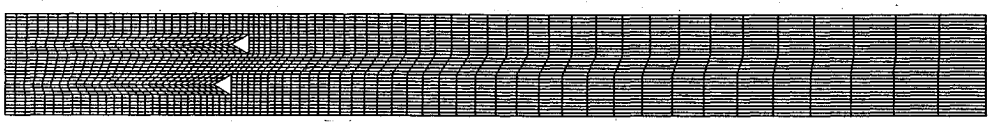

Fig. 12 Grid for the two-ring flame stabilizer.

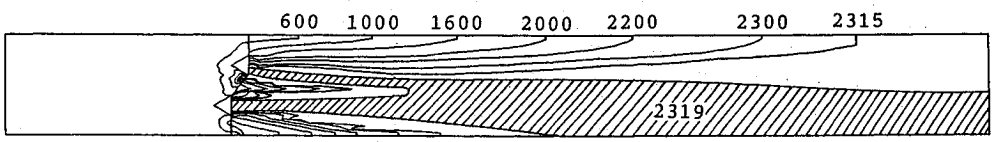

Fig. 13. Temperature contours of the two-ring flame stabilizer flow.

Summary

The results presented above demonstrate the capability of the current two-dimensional code developed for the simulation of gas turbine combustor flows. Emphasis in this study has been largely put on numerical aspects, such as nonstaggered body-fitted coordinate system, grid generation, an adaptive grid method, and a zonal grid method, etc. Several turbulence and combustion models have been assessed. Predictions of the backward-facing step flow, contoured wall combustor flow, and sudden expansion combustor flow, as well as flameholding flows have been conducted, the results are in general agreeable to the available experimental data.

Acknowledgments

This study is funded by the National Science Council of Taiwan, Republic of China under Contracts NSC78-0210-D006-01 and NSC80-0210-E006-05. Thanks are also due to the faculty and staff of the Department of Mechanical Engineering and Mechanics at Drexel University in Philadelphia for their help during the course of writing this manuscript when D. Lee stayed there as a visiting assistant professor in the fall of 1989.

References

[1]Shyy, W., Correa, S. M., and Braaten, M. E., "Computation of Flow in a Gas Turbine Combustor," *Combustion Science and Technology*, Vol. 58, Nos. 1–3, 1988, pp. 97–117.

[2]Priddin, C. H., and Coupland, J., "Impact of Numerical Methods on Gas Turbine Combustor Design and Development," *Combustion Science and Technology*, Vol. 58, Nos. 1–3, 1988, pp. 119–133.

[3]Sturgess, G. J., "Calculations of Aerospace Propulsion Combustor: A Review from Industry," *Calculations of Turbulent Reactive Flows*, Applied Mechanics Division, American Society for Mechanical Engineers, Vol. 81, 1986, pp. 185–232.

[4]Shyy, W., Braaten, M. E., and Burrus, D. L., "Study of Three-Dimensional Gas Turbine Combustor Flows," *International Journal Heat and Mass Transfer*, Vol. 32, No. 6, 1989, 1155–1164.

[5]Jones, W. P., and Launder, B. E., "The Prediction of Laminarization with a Two-Equation Model of Turbulence," *International Journal of Heat and Mass Transfer*, Vol. 15, No. 2, 1972, pp. 301–314.

[6]Launder, B. E., Reece, G. J., and Rodi, W., "Progress in the Development of a Reynolds Stresses Turbulence Closure," *Journal of Fluid Mechanics*, Vol. 68, Pt. 3, April 1975, pp. 537–566.

[7]Luboja, M., and Rodi, W., "Calculation of Turbulent Wall Jets with an Algebraic Reynolds Stress Model," *Journal of Fluids Engineering*, Vol. 102, No. 3, 1980, pp. 350–356.

[8]Nallasamy, M., "Turbulence Models and Their Applications to the Prediction of Internal Flows," *Computers and Fluids*, Vol. 15, No. 2, 1987, pp. 151–194.

[9]Autret, A., Grandotto, M., and Dekeyser, I., "Finite Element Computation of a Turbulent Flow over a Two-Dimensional Backward-Facing Step," *International Journal for Numerical Methods in Fluids*, Vol. 7, No. 2, 1987, pp. 89–102.

[10]Spalding, D. B., *Combustion and Mass Transfer*, Pergamon, London, 1979.

[11]Bilger, R. W., "Turbulent Flows with Nonpremixed Reactant," *Turbulent Reacting Flows*, edited by P. A. Libby and F. A. Williams, Springer-Verlag, New York, 1980, pp. 65–114.

[12]Naguib, A. S., "The Prediction of Axisymmetric Free Jet, Turbulent Reacting Flow," Ph.D. Dissertation, London Univ., London, 1974.

[13]Spalding, D. B., "Development of the Eddy-Break-Up Model of Tubulent Combustion," *16th Combustion Symposium (International)*, Combustion Inst., Pittsburgh, PA, 1976, pp. 1657–1663.

[14]Bray, K. N. C., "Turbulent Flows with Premixed Reactants," *Turbulent Reacting Flows*, edited by P. A. Libby and F. A. Williams, Springer-Verlag, New York, 1980, pp. 115–183.

[15]Patankar, S. V., *Numerical Heat Transfer and Fluid Flow*, Hemisphere, New York, 1980.

[16]Rhie, C. M., and Chow, W. L., "Numerical Study of the Turbulent Flow Past an Airfoil with Trailing Edge Separation," *AIAA Journal*, Vol. 21, No. 11, 1983, pp. 1525–1532.

[17]Lee, D., and Tsuei, Y. M., "LT-GRID, A Two-Dimensional Grid Generator" (in Chinese), Republic of China National Science Council Rept., CS75-0210-0006-04, Taiwan, ROC, 1987.

[18]Thompson, J. F., Warsi, Z. U. A., and Mastin, C. W., "Numerical Grid Generation," North Holland, Amsterdam, The Netherlands, 1985.

[19]Dwyer, H. A., Kee, R. J., and Sanders, B. R., "An Adaptive Grid Method for Problems in Fluid Mechanics and Heat Transfer," *AIAA Journal*, Vol. 18, No. 10, 1980, pp. 1205–1212.

[20]Lee, D., and Shyy, W., "A Study of One-Dimensional Transport Problem with Strong Convection and Source Terms," *Proceedings of the 18th Annual Pittsburgh Conference*, Univ. of Pittsburgh, Pittsburgh, PA, 1987, pp. 1845–1851.

[21]Lee, D., and Tsuei, Y. M., "A Modified Adaptive Grid Method for Recirculating Flows," *International Journal for Numerical Methods in Fluids*, Vol. 14, April 1992, pp. 775–792.

[22]Rai, M. M., "An Implicit Conservative, Zonal Boundaries Scheme for Euler Equation Calculations," *Computers and Fluids*, Vol. 14, No. 3, 1986, pp. 472–503.

[23]Lee, D., and Lin, J. S., "Computation of Nonreacting Flows of a Two-Ring Flame Stabilizer Using a Zonal Grid Method," *Numerical Heat Transfer*, Pt. A., Vol. 20, 1991, pp. 65–79.

[24]Lee, D., and Yeh, C. L., "Computation of Reacting Flame Stabilizer Flows Using a Zonal Grid Method," *Numerical Heat Transfer* (to be published).

[25]Jones, W. P., and Whitelaw, J. H., "Modelling and Measurements in Turbulent Combustion," *20th Combustion Symposium (International)*, Combustion Inst., Pittsburgh, PA, 1984, pp. 233–249.

[26]Khalil, E. E., *Modelling of Furnaces and Combustion*, Abacus Press, Tunbridge Wells, Kent, UK, 1982.

[27]Tennekes, H., and Lumley, J. L., "A First Course in Turbulence," MIT Press, Cambridge, MA, 1972.

[28]Amano, R. S., Goel, P., and Chai, J. C., "Turbulence Energy and Diffusion Transport of Third-Moments in a Separating and Reattaching Flow," *AIAA Journal*, Vol. 26, No. 3, 1988, pp. 273–282.

[29]Spalding, D. B., "Concentration Fluctuations in a Round Turbulent Free Jet," *Chemical Engineering Science*, Vol. 26, No. 1, 1971, pp. 95–107.

[30]Driver, M. D., and Seegmiller, H. L., "Features of a Reattaching Turbulent Shear Layer in Divergent Channel Flow," *AIAA Journal*, Vol. 23, No. 2, 1985, pp. 163–171.

[31]Lee, D., and Yeh, C. L., "Effects of Inlet Conditions on Computation of Flow over a Backward Facing Step," *Proceedings of 8th National Conference on Mechanical Engineering*, Chinese Society of Mechanical Engineering, Taipei, Taiwan, ROC, Dec. 1991, pp. 7–14.

[32]Ferziger, J. H., "Simulation of Incompressible Turbulent Flows," *Journal of Computational Physics*, Vol. 69, No. 1, 1987, pp. 1–48.

[33]Avva, R. K., Kline, S. J., and Ferziger, J. H., "Computations of Turbulent Flows over a Backward Facing Step—Zonal Approach," AIAA Paper 88-0611, 1988.

[34]Lee, D., and Chao, Y. C., "Numerical and Experimental Investigations of Gas Turbine Combustor Flows (III)" (in Chinese), National Science Council Rept., NSC80-0210-E006-05, Taiwan, ROC, Jan. 1992.

[35]McGuirk, J. J., and Rodi, W., "A Depth-Averaged Mathematical Model for the Near Field of Side Discharges into Open Channel Flow," *Journal of Fluid Mechanics*, Vol. 86, Pt. 4, June 1978, pp. 761–781.

[36]Lewis, M. H., and Smoot, L. D., "Turbulent Gaseous Combustion, Part I: Local Species Concentration Measurements," *Combustion and Flame*, Vol. 42, No. 2, 1981, pp. 183–196.

[37]Fujii, S., and Eguchi, K., "A Comparison of Cold and Reacting Flows Around a Bluff-Body Flame Stabilizer," *Journal of Fluids Engineering*, Vol. 103, No. 2, 1978, pp. 328–334.